

Study of highly-charged Ag-like and In-like ions for the development of atomic clocks and search for α -variation

M. S. Safronova^{1,2}, V. A. Dzuba³, V. V. Flambaum³, U. I. Safronova^{4,5}, S. G. Porsev^{1,6}, and M. G. Kozlov^{6,7}

¹*University of Delaware, Newark, Delaware, USA*

²*Joint Quantum Institute, NIST and the University of Maryland, College Park, Maryland, USA*

³*The University of New South Wales, Sydney, Australia*

⁴*University of Nevada, Reno, Nevada, USA*

⁵*University of Notre Dame, Notre Dame, Indiana, USA*

⁶*Petersburg Nuclear Physics Institute, Gatchina, Russia and*

⁷*St. Petersburg Electrotechnical University "LETI", St. Petersburg, Russia*

(Dated: March 2, 2022)

We carried out detailed high-precision study of Ag-like Nd^{13+} , Sm^{15+} and In-like Ce^{9+} , Pr^{10+} , Nd^{11+} , Sm^{13+} , Eu^{14+} highly-charged ions. These ions were identified to be of particular interest to the development of ultra-accurate atomic clocks, search for variation of the fine-structure constant α , and quantum information [Safronova et. al. Phys. Rev. Lett. 113, 030801 (2014)]. Relativistic linearized coupled-cluster method was used for Ag-like ion calculations, and a hybrid approach that combines configuration interaction and a variant of the coupled-cluster method was used for the In-like ion calculations. Breit and QED corrections were included. Energies, transition wavelengths, electric-dipole, electric-quadrupole, electric-octupole, magnetic-dipole, magnetic-quadrupole, magnetic-octupole reduced matrix elements, lifetimes, and sensitivity coefficients to α -variation were calculated. Detailed study of various contributions was carried out to evaluate uncertainties of the final results. Energies for several similar “reference” ions, where the experimental values are available were calculated and compared with experiment for further tests of the accuracy.

I. INTRODUCTION

The modern theories aimed at unifying gravitation with the three other fundamental interactions suggest variation of the fundamental constants in an expanding universe [1]. A very large recent study of quasar absorption systems may indicate a spatial variation in the fine-structure constant $\alpha = e^2/\hbar c$ [2]. Spatial α -variation hypothesis can be tested in terrestrial studies if sensitivity $\delta\alpha/\alpha \sim 10^{-19} \text{ yr}^{-1}$ is achieved [3, 4]. Development of ultra-precise atomic clocks already allowed laboratory tests of the temporal α -variation at the present time. Different optical atomic clocks use transitions that have different contributions of the relativistic corrections to frequencies. Therefore, comparison of these clocks can be used to search for α -variation. The most precise laboratory test of temporal α -variation has been carried out at NIST [5] by measuring the frequency ratio of Al^+ and Hg^+ optical atomic clocks with a fractional uncertainty of 5.2×10^{-17} . Repeated measurements during the year yielded a constraint on the temporal variation of α of $\dot{\alpha}/\alpha = (-1.6 \pm 2.3) \times 10^{-17}$. Development of ultra-precise atomic clocks is also essential for various other tests of fundamental physics, development of extremely sensitive quantum-based tools, very-long-baseline interferometry for telescope array synchronization, and tracking of deep-space probes [6, 7].

Certain systems exhibit much higher sensitivity to the variation of α allowing more precise tests of the temporal variation and possible tests of the spatial variation of α [2]. Selected transitions in highly-charged ions (HCI) were shown to have very large sensitivities to α -variation owing to high nuclear charge Z , high ionization state,

and differences in the configuration composition of the corresponding states [8, 9]. While highly-charged ions have very large ionization energies, some of these systems have transitions that lie in the optical range due to level crossing. Moreover, these ions have very long-lived low-lying metastable states which is a first requirement for the development of a frequency standard. Highly-charged ions are less sensitive to external perturbations than either neutral atoms or singly charged ions due to more compact size of the electronic cloud. As a result, some of the usual systematic clock uncertainties as well as decoherence processes in quantum information applications may be suppressed.

Ag-like Nd^{13+} and Sm^{15+} were proposed for the development of atomic clocks and subsequent tests of the variation of the fine-structure constant in Refs. [10, 11]. Detailed study of the potential clock uncertainties with these systems [12] have shown that the fractional accuracy of the transition frequency in the clocks based on highly-charged ions can be smaller than 10^{-19} . Estimated sensitivity to the variation of α for highly-charged ions approaches 10^{-20} per year [10], which may allow for tests of spatial variation of the fine-structure constants that may be indicated by the observational studies [2]. In-like Ce^{9+} , Pr^{10+} , Nd^{11+} and Sm^{13+} were proposed for the applications listed above in Ref. [11]. Experimental work in HCIs requires knowledge of many atomic properties of these systems, especially, wavelengths, transition rates, and lifetimes. To the best of our knowledge, no transition rates or lifetimes have been measured for any of the HCIs studied in this work. The energy levels have only been measured for Nd^{13+} , Sm^{15+} , and Ce^{9+} . No experimental data at all exist for Pr^{10+} , Nd^{11+} , Sm^{13+} ,

and Eu^{14+} . Accurate theoretical predictions of the transition wavelengths for these systems are particularly difficult owing to severe cancellations of upper and lower state energies, and we use the most high-precision methods available to perform the calculations.

In this work, we carried out detailed high-precision study of Ag-like Nd^{13+} and Sm^{15+} and In-like Ce^{9+} , Pr^{10+} , Nd^{11+} , Sm^{13+} , and Eu^{14+} highly-charged ions using a relativistic linearized coupled-cluster method and a hybrid approach that combines configuration interaction and a variant of the coupled-cluster method. Breit and QED corrections were included into the calculations. Key results were presented in Ref. [11]. Our calculations include energies, transition wavelengths, electric-dipole, electric-quadrupole, electric-octupole, magnetic-dipole, magnetic-quadrupole, magnetic-octupole transition rates, lifetimes, and sensitivity coefficients to α -variation q and K . We carried out extensive study of the uncertainties of our results. Three independent methods were used for the uncertainty studies:

- Energies of Nd^{13+} , Sm^{15+} , and In-like Ce^{9+} as well as several similar “reference” ions Cs^{6+} , Ba^{7+} , and Ba^{9+} , where the experimental values are available, were calculated and compared with experiment.
- For three of the In-like Ce^{9+} , Pr^{10+} , and Nd^{11+} “monovalent” ions, both of the approaches used in this work are applicable so we were able to compare the various properties calculated with both methods to study the accuracy of the calculations.
- Detailed study of higher-order, Breit, QED, and higher partial wave contributions was carried out to evaluate uncertainties of the final results for each ion.

We start with the brief description of the methods used in this work in Section II. The results for Ag-like and In-like ions are presented in Sections III and IV, respectively.

II. METHODS

We use two different relativistic high-precision approaches for all of the calculations carried out in this work. The first approach is the relativistic linearized coupled-cluster method that includes all single, double, and partial triple excitations (SDpT) of Dirac-Fock wave function [13]. It is applicable only to monovalent systems, so we use it for the calculation of properties of Ag-like ions and those In-like ions that can be treated as monovalent systems. SDpT has been extremely successfully in predicting properties of alkali-metal atoms and other monovalent ions [13].

A. Monovalent systems: all-order SDpT method

The Ag-like ions have a single valence electron above the closed $1s^2 2s^2 2p^6 3s^2 3p^6 3d^{10} 4s^2 4p^6 4d^{10}$ core. It allows us to use relativistic linearized coupled-cluster method that includes all single, double, and partial triple excitations of Dirac-Fock wave function. We refer the reader to the review [13] for detail description of the method and its applications and give only a brief introduction to this approach.

The point of departure in all our calculations is the relativistic no-pair Hamiltonian $H = H_0 + V_I$ [14] expressed for the case of *frozen-core* V^{N-1} Dirac-Fock potential as

$$H_0 = \sum_i \epsilon_i : a_i^\dagger a_i :, \quad (1)$$

$$V_I = \frac{1}{2} \sum_{ijkl} g_{ijkl} : a_i^\dagger a_j^\dagger a_l a_k :, \quad (2)$$

where g_{ijkl} are two-particle matrix elements of the Coulomb interaction, ϵ_i in Eq. (1) is the eigenvalue of the Dirac equation, a_i^\dagger , a_i are creation and annihilation operators, and $: :$ designate normal ordering of operators with respect to the core.

In the linearized coupled-cluster SDpT approach the atomic wave function of a monovalent atom in a state v is given by an expansion

$$|\Psi_v\rangle = \left[1 + \sum_{ma} \rho_{ma} a_m^\dagger a_a + \frac{1}{2} \sum_{mnab} \rho_{mnab} a_m^\dagger a_n^\dagger a_b a_a + \sum_{m \neq v} \rho_{mv} a_m^\dagger a_v + \sum_{mnva} \rho_{mnva} a_m^\dagger a_n^\dagger a_a a_v + \frac{1}{6} \sum_{mnrab} \rho_{mnrab} a_m^\dagger a_n^\dagger a_r^\dagger a_b a_a a_v \right] a_v^\dagger |\Psi_C\rangle. \quad (3)$$

Here indices a and b range over all occupied core states while the indices m , n , and r range over all possible virtual states, and $|\Psi_C\rangle$ is the lowest-order frozen-core wave function. The quantities ρ_{ma} , ρ_{mv} are single-excitation coefficients for core and valence electrons; ρ_{mnab} and ρ_{mnva} are core and valence double-excitation coefficients, respectively. The triple excitations ρ_{mnrab} are included perturbatively into the energy and single-valence excitation coefficient equations. In the single-double (SD) variant of the all-order method, only single and double excitations are included.

The equations for the excitation coefficients ρ and the correlation energy are derived by substituting the state vector $|\Psi_v\rangle$ into the many-body Schrödinger equation $H|\Psi_v\rangle = E|\Psi_v\rangle$. The resulting system of equations is solved iteratively until the correlation energy converges to required numerical accuracy. This approach includes dominant many-body perturbation theory (MBPT) terms to all orders because every iteration picks up correlation terms that correspond to the next order of perturbation theory.

TABLE I: Second-order Coulomb correlation energy calculated with $l_{\max} = 5$, $l_{\max} = 6$, and final extrapolated values (Final). The contributions of $l = 6$ and $l > 6$ are compared in the last two columns. All values are in cm^{-1} .

Level	$l_{\max} = 5$	$l_{\max} = 6$	Final	$l = 6$	$l > 6$
5s	-22140	-22402	-22672	-262	-270
5p _{1/2}	-20451	-20710	-20989	-259	-278
5p _{3/2}	-19136	-19375	-19632	-239	-257
4f _{5/2}	-26474	-27931	-29418	-1456	-1488
4f _{7/2}	-26044	-27493	-28971	-1449	-1478

The matrix elements of any one-body operator $Z = \sum_{ij} z_{ij} a_i^\dagger a_j$, such as transition operators Ek and Mk , $k = 1, 2, 3$ needed for this work, are obtained within the framework of the all-order method as

$$Z_{wv} = \frac{\langle \Psi_w | Z | \Psi_v \rangle}{\sqrt{\langle \Psi_v | \Psi_v \rangle \langle \Psi_w | \Psi_w \rangle}} = \frac{z_{wv} + Z^{(a)} + \dots + Z^{(t)}}{\sqrt{\langle \Psi_v | \Psi_v \rangle \langle \Psi_w | \Psi_w \rangle}}, \quad (4)$$

where $|\Psi_v\rangle$ and $|\Psi_w\rangle$ are given by the expansion (3) restricted to SD approximation. The terms $Z^{(a)} \dots Z^{(t)}$ are linear or quadratic functions of the excitation coefficients and z_{wv} is the DF matrix element [15].

We use a complete set of DF wave functions on a non-linear grid generated using B-splines constrained to a spherical cavity $R = 60$ a.u. The basis set consists of 50 splines of order 9 for each value of the relativistic angular quantum number κ .

The Breit interaction is included in the construction of the basis set. The QED radiative corrections to energy levels are included using the method described in [16]. The contribution of the QED corrections for the ions calculated in this work is only significant for the configurations that contain valence 5s state. Therefore, the QED can be omitted for ions where none of the low-lying configurations contain 5s valence state.

The partial waves with $l_{\max} = 6$ are included in all internal summations over all excited states. We find that inclusion of the higher partial waves with $l > 6$ is very important for accurate description of the 4f states. We use second-order perturbation theory where we can extrapolate the result to $l_{\max} = \infty$ to evaluate the contribution of $l > 6$. The results are illustrated in Table I where we list second-order Coulomb correlation energies calculated with $l_{\max} = 5$ and $l_{\max} = 6$, their difference which is the contribution of $l = 6$, and the final results calculated with $l = 10$ partial waves and extrapolated to account for $l > 10$ contributions. The difference of the final and $l_{\max} = 6$ results gives the contribution of the $l > 6$ partial waves (last column). We find that it is remarkably close to the contribution of the $l = 6$ partial wave. The second order dominates correlation energy, therefore, this empirical rule is expected to hold for the all-order correlation corrections. As a result, we estimate the effect

of higher partial waves in all of the calculations in this work by carrying out the entire all-order calculation with $l_{\max} = 5$ and $l_{\max} = 6$ and adding the difference to the final result. We label this contribution ‘‘Extrap’’ in all tables below.

B. Multivalent systems: CI+all-order method

The linearized coupled-cluster method used for Ag-like ions is not directly applicable for systems with two or more valence electrons. We use a hybrid method that combines the modified linearized single-double (SD) coupled-cluster method with configuration approach developed in [19, 20]. The CI many-electron wave function is obtained as a linear combination of all distinct states of a given angular momentum J and parity [21]:

$$\Psi_J = \sum_i c_i \Phi_i. \quad (5)$$

Then, energies and wave functions of low-lying states are determined by diagonalizing the effective Hamiltonian:

$$H^{\text{eff}} = H_1 + H_2, \quad (6)$$

where H_1 and H_2 represents the one-body and two-body parts of the Hamiltonian, respectively. The matrix elements and other properties, such as electric-multipole and magnetic-multipole transition matrix elements, can be determined using the resulting wave functions.

The CI + many-body perturbation theory (MBPT) approach developed in [21] allows one to incorporate core excitations in the CI method by including perturbation theory terms into an effective Hamiltonian (6). Then, the one-body part H_1 is modified to include the correlation potential Σ_1 that accounts for part of the core-valence correlations:

$$H_1 \rightarrow H_1 + \Sigma_1. \quad (7)$$

and the two-body Coulomb interaction term H_2 is modified by including the two-body part of core-valence interaction that represents screening of the Coulomb interaction by valence electrons;

$$H_2 \rightarrow H_2 + \Sigma_2. \quad (8)$$

The CI method is then applied as usual with the modified H^{eff} to obtain improved energies and wave functions. In the CI + all-order approach, the corrections to the effective Hamiltonian Σ_1 and Σ_2 are calculated using a modified version of the linearized coupled-cluster all-order method described above which allows to include dominant core and core-valence correlation corrections to the effective Hamiltonian to all orders. The detailed description of the CI+all-order method and all formulas are given in [20]. Since the CI space includes only three valence electrons for In-like ions, it can be made essentially complete. The CI+all-order method yielded accurate wave functions for the calculations of such atomic

TABLE II: Energies of Ag-like Ba^{9+} , Nd^{13+} , and Sm^{15+} ions relative to the ground state evaluated in the SDpT all-order approximation (in cm^{-1}). Contributions from higher-order Coulomb correlation (above second-order MBPT), estimated contributions of higher partial waves (above $l > 6$), Breit interaction, and QED are given separately in columns HO, Extrap, Breit, and QED, respectively. Experimental results are from [17] for Ba^{9+} and [18] for Nd^{13+} and Sm^{15+} . Differences with experiment are given in cm^{-1} and % in columns “Diff.” and “Diff.%”. Wavelengths for transitions to the ground state are given in the last two columns in nm.

Ion	Level	Expt.	Ref. [10]	MBPT2	HO	Extrap	Breit	QED	Final	Diff.	Diff.%	λ_{th}	λ_{expt}
Ba^{9+}	$5s_{1/2}$	0		0	0	0	0	0	0				
	$5p_{1/2}$	139348		140221	-719	-18	304	-530	139258	90	0.06%	71.81	71.76
	$5p_{3/2}$	166361		167744	-950	-2	-24	-483	166285	76	0.05%	60.14	60.11
	$4f_{5/2}$	222558		224696	139	-1006	-912	-569	222350	208	0.09%	44.97	44.93
	$4f_{7/2}$	224074		226433	57	-997	-1079	-560	223856	218	0.10%	44.67	44.63
Nd^{13+}	$5s_{1/2}$	0	0	0	0	0	0	0	0				
	$4f_{5/2}$	55870	58897	58596	761	-1247	-1421	-983	55706	164	0.29%	179.5	179.0
	$4f_{7/2}$	60300	63613	63429	671	-1238	-1767	-961	60134	166	0.28%	166.3	165.8
	$5p_{1/2}$	185066		185876	-492	-33	560	-883	185028	38	0.02%	54.05	54.03
	$5p_{3/2}$	234864		236463	-74	7	-14	-801	234887	-23	-0.01%	42.57	42.58
Sm^{15+}	$4f_{5/2}$	0	0	0	0	0	0	0	0				
	$4f_{7/2}$	6555	6806	6949	-92	9	-454	31	6444	111	1.69%	1552	1526
	$5s_{1/2}$	60384	55675	57100	-820	1316	1686	1236	60517	-133	-0.22%	165.2	165.6
	$5p_{1/2}$	268488		266011	-1218	1277	2398	138	268604	-116	-0.04%	37.23	37.25
	$5p_{3/2}$	333203		331659	-1482	1297	1870	243	333385	-182	-0.05%	29.99	30.01

properties as lifetimes, polarizabilities, hyperfine structure constants, etc. for a number of divalent systems and Tl [20, 22–27]. We refer the reader to Refs. [13, 28, 29] and [20, 22–24, 26, 27] for detailed descriptions of the linearized coupled-cluster and CI+all-order methods, respectively. We use both methods for In-like ions with the exception of Sm^{13+} and Eu^{14+} that have low-lying trivalent configurations, such as $4f^25s$ as an additional test of accuracy.

As in the monovalent all-order method, we included the Breit interaction on the same footing as the Coulomb interaction in the basis set, which incorporates higher-order Breit effects. The Gaunt part of the Breit interaction is included in the CI. The contribution of the $l > 6$ partial waves is calculated as described above, i.e. using the empirical result that total $l > 6$ extrapolated contribution is approximately equal to the $l = 6$ contribution. To evaluate the uncertainty of our calculations, we carried out several calculations for each ion to separate the contributions of the higher-order Coulomb correlation, Breit, QED, and $l > 6$ higher partial waves. Several methods are developed to evaluate the uncertainties.

The sensitivity of the atomic transition frequency ω to the variation of the fine-structure constant α can be quantified using a coefficient q defined as

$$\omega(x) = \omega_0 + qx, \quad (9)$$

where

$$x = \left(\frac{\alpha}{\alpha_0}\right)^2 - 1. \quad (10)$$

In the equation above, the frequency ω_0 corresponds to the value of the fine-structure constant α_0 at some initial

point in time. It is preferable to select transitions with significantly different values of q , since the ratio of two frequencies, which is a dimensionless quantity, is studied over time in the experiment. Extra enhancement will be present if q for these transitions have different signs. We also define a dimensionless enhancement factor $K = 2q/\omega$.

The calculation of sensitivity coefficient q requires a performance of three calculations with different values of α for every ion considered in this work. First, the calculation is carried out with the current CODATA value of α [30]. Next, two other calculations are performed with α^2 varied by $\pm 1\%$. The value of q is then determined as a numerical derivative

$$q = \frac{\omega(0.01) - \omega(-0.01)}{0.02}, \quad (11)$$

where $\omega(\pm 0.01)$ are results of the calculations with α^2 varied by $\pm 1\%$, respectively. The other calculation (with CODATA value of α) is used to verify that the change in ω is very close to linear. We also carried out test calculation for one of the ions, Pr^{10+} , with changing α^2 by $\pm 5\%$ and obtained results identical to the ones obtained with $\pm 1\%$ change.

The lifetime of a state a is calculated as

$$\tau_a = \frac{1}{\sum_b A_{ab}}.$$

The multipole transition rates A_{ab} are determined using

TABLE III: Energies and sensitivity coefficients q for Ag-like ions relative to the ground state evaluated in the SDpT all-order approximation in cm^{-1} ; $K = 2q/\omega$ is the enhancement factor. Lowest-order DF sensitivity coefficients q are given for comparison.

Ion	Level	Energy	q (DF)	q (SDpT)	K
Nd^{13+}	$5s_{1/2}$	0	0	0	
	$4f_{5/2}$	55706	102609	104229	3.7
	$4f_{7/2}$	60134	106276	108243	3.6
	$5p_{1/2}$	185028	16047	15953	0.2
	$5p_{3/2}$	234887	71013	72079	0.6
Sm^{15+}	$4f_{5/2}$	0	0	0	
	$4f_{7/2}$	6444	5536	5910	1.8
	$5s_{1/2}$	60517	-132449	-134148	-4.4
	$5p_{1/2}$	268604	-113153	-114999	-0.9
	$5p_{3/2}$	333385	-40883	-41477	-0.2

the formulas:

$$A(E1) = \frac{2.02613 \times 10^{18}}{(2J_a + 1)\lambda^3} S(E1), \quad (12)$$

$$A(M1) = \frac{2.69735 \times 10^{13}}{(2J_a + 1)\lambda^3} S(M1), \quad (13)$$

$$A(E2) = \frac{1.11995 \times 10^{18}}{(2J_a + 1)\lambda^5} S(E2), \quad (14)$$

$$A(M2) = \frac{1.49097 \times 10^{13}}{(2J_a + 1)\lambda^5} S(M2), \quad (15)$$

$$A(E3) = \frac{3.14441 \times 10^{17}}{(2J_a + 1)\lambda^7} S(E3), \quad (16)$$

$$A(M3) = \frac{4.18610 \times 10^{12}}{(2J_a + 1)\lambda^7} S(M3), \quad (17)$$

where the wavelength λ is in \AA and the line strength S is in atomic units.

III. AG-LIKE IONS

The $5s - 4f$ level crossing (i.e. change of the level order) in Ag-like isoelectronic sequence happens from Nd^{13+} to Sm^{15+} . The order of the first few levels for previous ions, such as Ba^{9+} is $5s$, $5p$, and $4f$. The ordering becomes $5s$, $4f$, $5p$ for Nd^{13+} and then finally switches to $4f$, $5s$, $5p$ for Sm^{15+} . The Pm^{14+} has no stable isotopes and we do not list its energies here. However, we find that the $5s$ and $4f_{5/2}$ states are separated by only about 300 cm^{-1} .

We list the energies of Ag-like Ba^{9+} , Nd^{13+} , and Sm^{15+} ions relative to the ground state evaluated in the SDpT all-order approximation in Table II (in cm^{-1}). Since the experimental energies are available for Nd^{13+} and Sm^{15+} , Ag-like ions represent excellent benchmark systems for our calculations. While Ba^{9+} is not of practical interest

for applications of this work, experimental data are available for Ag-like and In-like Ba ions. Therefore, we carried out calculations for these Ba ions to provide similar reference systems. The total of lowest-order DF and second order values are given in column labelled “MBPT2”. Contributions from higher-order Coulomb correlation, estimated contributions of higher partial waves (above $l > 6$), Breit interaction, and QED are given separately in columns HO, Extrapol, Breit, and QED. The higher-order corrections are calculated as the difference of the all-order and the second-order results. All all-order calculations include partial triple excitations as described above. The Breit contribution is calculated as the difference of the energies obtained with and without the inclusion of the Breit interactions. The QED radiative corrections to energy levels are included using the method described in [16].

Experimental results are from [17] for Ba^{9+} and [18] for Nd^{13+} and Sm^{15+} . Difference with experiment is given in cm^{-1} and % in columns “Diff.” and “Diff.%”. Wavelengths for transitions to the ground state are given in last two columns in nm. Our results are in excellent agreement with experimental data. We also include comparisons with recent correlation potential method results of Ref. [10]. The table illustrates that inclusion of Breit, higher-order partial waves, and QED contributions is essential for achieving accurate results.

The sensitivity coefficients q for Ag-like ions obtained as described in Section II are given in Table III. Lowest-order DF and final SDpT all-order sensitivity coefficients q are given for comparison. The Breit interaction is included and QED is omitted in the calculation of q factors. Final SDpT all-order transition energies are given for reference. All energy and q values are given relative to the ground state in cm^{-1} . SDpT energies and q coefficients are used to calculate enhancement factors $K = 2q/\omega$ given in the last column of the table. For consistency, we use our final theoretical values of energies to calculate K for all ions considered in this work. We find that while the correlation correction is very important for accurate calculation of the transition energies, it only weakly affects the values of q . The DF values differ from the final all-order values of q by less than 2% with the exception of the $4f_{5/2} - 4f_{7/2}$ transition in Sm^{15+} , where the transition energy is relatively small and correlation contributes 6.3%. The enhancement factors are large for the $5s - 4f$ transitions for both ions.

Lowest order (Z^{DF}) and all-order (Z^{SDpT}) multipole matrix elements E_k and M_k , $k = 1, 2, 3$ in a.u. and corresponding transition rates A (in s^{-1}) are given in Table IV. The transition rates are calculated using the formulas in Section II. Experimental energies from Ref. [18] are used in transition rate calculations. The experimental energies (in cm^{-1}) and wavelengths (in nm) from Ref. [18] are listed in Table IV. The lifetimes are given in the same row as the level designation for the convenience of presentation. A single transition gives the dominant contribution to the lifetimes of Nd^{13+} states considered in this work.

TABLE IV: Lowest order (Z^{DF}) and all-order (Z^{SDpT}) multipole matrix elements Ek and Mk , $k = 1, 2, 3$ in a.u., transition rates A (in s^{-1}), and lifetimes in Ag-like ions. Experimental energies from Ref. [18] are used in calculation of transition rates. Energies (in cm^{-1}) and wavelengths (in nm) are listed for reference. The numbers in brackets represent powers of 10.

Level	Transition	Energy	λ	Z^{DF}	Z^{SDpT}	A	Lifetime
Ag-like Nd^{13+}							
$4f_{5/2}$	$4f_{5/2} - 5s_{1/2}$	E3	55870	179.1	0.955	7.568[-07]	15.3 days
	$4f_{5/2} - 5s_{1/2}$	M2	55870	179.0	0.00004	1.987[-11]	
$4f_{7/2}$	$4f_{7/2} - 4f_{5/2}$	M1	4430	2257	1.850	1.004	0.996 s
	$4f_{7/2} - 4f_{5/2}$	E2	4430	2257	0.320	1.936[-06]	
	$4f_{7/2} - 5s_{1/2}$	E3	60300	165.8	1.113	1.319[-06]	
$5p_{1/2}$	$5p_{1/2} - 5s_{1/2}$	E1	185066	54.03	1.018	4.899[09]	0.204 ns
$5p_{3/2}$	$5p_{3/2} - 5s_{1/2}$	E1	234864	42.58	1.446	1.016[10]	0.0984 ns
Ag-like Sm^{15+}							
$4f_{7/2}$	$4f_{7/2} - 4f_{5/2}$	M1	6555	1525.6	1.850	3.251	0.308 s
	$4f_{7/2} - 4f_{5/2}$	E2	6555	1525.6	0.256	8.801[-06]	
$5s_{1/2}$	$5s_{1/2} - 4f_{5/2}$	E3	60384	165.6	0.676	1.986[-06]	3.62 days
	$5s_{1/2} - 4f_{7/2}$	E3	53829	185.8	0.789	1.214[-06]	
	$5s_{1/2} - 4f_{5/2}$	M2	60384	165.6	0.00004	3.643[-11]	
$5p_{1/2}$	$5p_{1/2} - 5s_{1/2}$	E1	208104	48.05	0.940	5.978[09]	0.167 ns
$5p_{3/2}$	$5p_{3/2} - 5s_{1/2}$	E1	272819	36.65	1.337	1.368[10]	0.0731 ns

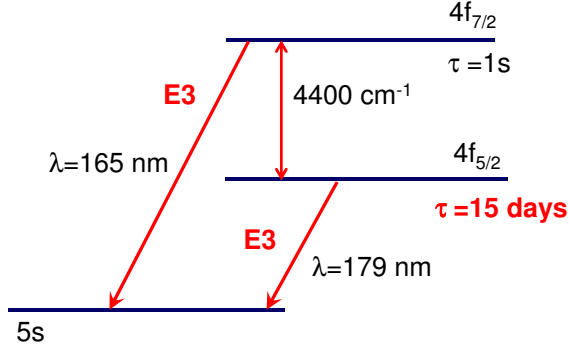


FIG. 1: Energy levels and radiative lifetimes of low-lying levels of Ag-like Nd^{13+} .

The strongest transition from the metastable $4f_{5/2}$ level of this ion is E3, resulting in the extremely long lifetime of more than 15 days. Therefore, this system may be considered to have two ground states. The low-lying levels of Nd^{13+} ion and our estimates of the radiative lifetimes are shown in Fig. 1 for illustration. Long lifetimes of Nd^{13+} ion and large values of q make it particularly attractive candidate for applications considered in this work.

There are two significant contributions to the lifetime of the $5s$ state in Sm^{15+} , $5s - 4f_{5/2}$ and $5s - 4f_{7/2}$, both of which are E3 transitions. The $5s - 4f_{5/2}$ M2 transition gives negligible contribution. The $5s$ state has also extremely long lifetime, 3.6 days, but has two decay channels.

The sensitivity of transitions in Nd^{13+} and Sm^{15+} to variation of α as well as uncertainty budget of the atomic

clocks were discussed in detail in Ref. [10]. Blackbody radiation shift, Zeeman shift, electric quadrupole shift, and other perturbations affecting clock frequencies were considered in [10] and the ultimate fractional frequency uncertainty was projected at 10^{-19} .

IV. IN-LIKE IONS

In-like ions have two more valence electrons in comparison with Ag-like ions, and in general are considered to be trivalent systems. However, the states with $5s^2nl$ valence configurations above $1s^22s^22p^63s^23p^63d^{10}4s^24p^64d^{10}$ core may be considered to be monovalent with $5s^2$ shell included into the core. These ions may be treated with both monovalent coupled-cluster SDpT all-order method and many-electron CI+all-order method. We use both of these approaches and compare their accuracy. The accuracy of these methods for neutral Tl and In has been recently discussed in Refs. [32, 33]. The trivalent $4f^3$ and $4f^25s$ configurations in Sm^{13+} and Eu^{14+} can only be treated with the CI+all-order method.

There are two level crossings of interest for the present work in In-like isoelectronic sequence, $5p - 4f$ and $4f - 5s$. The first one happens for Pr^{10+} and Nd^{11+} and leads to change of level order from $5p$, $4f$ to $4f$, $5p$. Pr^{10+} represents a particularly attractive case where both $4f_j$ levels are located between the $5p_{1/2}$ and $5p_{3/2}$ fine structure multiplet, making $4f_{5/2}$ a very long-lived metastable level.

Energies of In-like “monovalent” Cs^{6+} , Ba^{7+} , Ce^{9+} , Pr^{10+} , and Nd^{11+} ions relative to the ground state are

TABLE V: Energies of In-like “monovalent” Cs^{6+} , Ba^{7+} , Ce^{9+} , Pr^{10+} , and Nd^{11+} ions relative to the ground state in cm^{-1} . Results of two different methods, monovalent coupled-cluster SDpT and CI+all-order, are given in columns labeled SDpT and CI+all. The CI+all-order results are taken as final. Contributions from higher-order Coulomb correlation (difference of the CI+MBPT and CI+all-order calculations), estimated contributions of higher partial waves (above $l > 6$), and Breit interaction are given separately in columns HO, Extrap, and Breit, respectively. Experimental results are from [17] for Cs^{6+} and Ba^{7+} and from [31] for Ce^{9+} . Differences with experiment are given in cm^{-1} and % in columns “Diff.” and “Diff.%”. Estimated uncertainties of theoretical calculations are given in column “Unc”. Wavelengths for transitions to the ground state are given in last two columns in nm.

Ion	Level	Expt	SDpT	Diff.	CI+MBPT	HO	Extrap	Breit	CI+all	Unc.	Diff.	Diff.%	λ_{th}	λ_{expt}
Cs^{6+}	$5p_{1/2}$	0	0	0	0	0	0	0	0					
	$5p_{3/2}$	19379	19351	28	19733	-127	11	-245	19372		7	0.04	516.20	516.01
	$4f_{5/2}$	166538	166851	-313	166341	1839	-740	-995	166446		92	0.06	60.08	60.05
	$4f_{7/2}$	167297	167603	-306	167234	1787	-733	-1103	167186		111	0.07	59.81	59.77
Ba^{7+}	$5p_{1/2}$	0	0	0	0	0	0	0	0					
	$5p_{3/2}$	23592	23564	28	24020	-134	12	-293	23605		-13	-0.05	423.65	423.87
	$4f_{5/2}$	137385	137770	-385	137086	2224	-858	-1197	137256		129	0.09	72.86	72.79
	$4f_{7/2}$	138675	139043	-368	138570	2169	-851	-1345	138542		133	0.10	72.18	72.11
Ce^{9+}	$5p_{1/2}$	0	0	0	0	0	0	0	0					
	$5p_{3/2}$	33427	33406	21	33986	-147	14	-403	33450	130	-23	-0.07	299.0	299.2
	$4f_{5/2}$	54947	55419	-472	54601	2687	-1011	-1595	54683	220	264	0.48	182.9	182.0
	$4f_{7/2}$	57520	57968	-448	57441	2628	-1004	-1830	57235	310	285	0.50	174.7	173.9
Pr^{10+}	$5p_{1/2}$		0		0	0	0	0	0					
	$4f_{5/2}$		3958		3471	2821	-1063	-1797	3702 ^a	200			2700(140)	
	$4f_{7/2}$		7276		7136	2761	-1057	-2079	7031 ^a	200			1422(40)	
	$5p_{3/2}$		39084		39745	-154	14	-464	39141	40			255.5(3)	
Nd^{11+}	$4f_{5/2}$		0		0	0	0	0	0					
	$4f_{7/2}$		4155		4566	-61	7	-332	4180	100			2392(60)	
	$5p_{1/2}$		52823		53491	-2916	1106	2003	53684	500			186.3(1.7)	
	$5p_{3/2}$		98175		99549	-3076	1121	1472	99066	500			100.9(5)	

^aThese values are adjusted by 270 cm^{-1} based on the comparison of Ce^{9+} results with experiment.

TABLE VI: Comparison of sensitivity coefficients q in In-like Pr^{10+} ions relative to the ground state evaluated in the lowest-order Dirac-Fock (DF+Breit), SDpT, and CI+all-order approximation in cm^{-1} . The second-column (DF) shows lowest-order results without the Breit interaction. Breit is included in all other calculation.

Level	DF	DF+Breit	SDpT	CI+all
$5p_{1/2}$	0	0	0	0
$4f_{5/2}$	75276	73494	73865	73849
$4f_{7/2}$	78081	76059	76803	76833
$5p_{3/2}$	44552	43977	44091	44098

given in Table V in cm^{-1} . We calculate the energies for all three Cs^{6+} , Ba^{7+} , Ce^{9+} ions where the experimental values are available to understand the trends of the difference with experiment so we can improve the values and reduce the uncertainty of the Pr^{10+} energies. Results of two different methods, monovalent coupled-cluster SDpT and CI+all-order, are given in columns labeled SDpT and CI+all. Difference with experiment is given in cm^{-1} and % in columns “Diff.” and “Diff.%”. The table clearly

TABLE VII: Energies and sensitivity coefficients q for In-like ions relative to the ground state evaluated in the CI+all-order approximation in cm^{-1} ; $K = 2q/\omega$ is the enhancement factor.

Ion	Level	Energy	q	K
Ce^{9+}	$5p_{1/2}$	0	0	
	$5p_{3/2}$	33450	37544	2.2
	$4f_{5/2}$	54683	62873	2.3
	$4f_{7/2}$	57235	65150	2.3
Pr^{10+}	$5p_{1/2}$	0	0	
	$4f_{5/2}$	3702	73849	40
	$4f_{7/2}$	7031	76833	22
	$5p_{3/2}$	39141	44098	2.3
Nd^{11+}	$4f_{5/2}$	0	0	
	$4f_{7/2}$	4180	3785	1.8
	$5p_{1/2}$	53684	-85692	-3.2
	$5p_{3/2}$	99066	-34349	-0.7

illustrates that the CI+all-order method gives the results in better agreement with experiment. Therefore, the CI+all-order results are taken as final for all five ions

TABLE VIII: Lowest order (Z^{DF}) and all-order (Z^{SDPT}) multipole matrix elements $E2$ and $M1$, transition rates A (in s^{-1}), and lifetimes in In-like ions. Experimental energies from Refs. [17, 31] are used for Cs^{6+} , Ba^{7+} , and Ce^{9+} ions; theoretical energies from Table V are used for Pr^{10+} and Nd^{11+} . Energies (in cm^{-1}) and wavelengths (in nm) are listed for reference. The numbers in brackets represent powers of 10.

Level	Transition		Energy	λ	Z^{DF}	Z^{SDPT}	A	Lifetime
In-like Cs ⁶⁺								
5p _{3/2}	5p _{3/2} − 5p _{1/2}	M1	19379	516.0	1.152	1.152	6.510[01]	1.52[-02] s
	5p _{3/2} − 5p _{1/2}	E2	19379	516.0	3.100	2.885	6.371[-01]	
4f _{5/2}	4f _{5/2} − 5p _{1/2}	E2	166538	60.05	2.608	2.315	1.282[04]	6.71[-05] s
	4f _{5/2} − 5p _{3/2}	E2	147159	67.95	1.416	1.271	2.080[03]	
4f _{7/2}	4f _{7/2} − 4f _{5/2}	M1	759	13175	1.851	1.851	5.053[-03]	1.03[-04] s
	4f _{7/2} − 4f _{5/2}	E2	759	13175	0.970	0.784	2.166[-09]	
	4f _{7/2} − 5p _{3/2}	E2	147918	67.61	3.486	3.123	9.668[03]	
In-like Ba ⁷⁺								
5p _{3/2}	5p _{3/2} − 5p _{1/2}	M1	23592	423.9	1.152	1.151	1.174[02]	8.43[-03] s
	5p _{3/2} − 5p _{1/2}	E2	23592	423.9	2.725	2.544	1.324[00]	
4f _{5/2}	4f _{5/2} − 5p _{1/2}	E2	137385	72.79	1.984	1.770	2.862[03]	3.13[-04] s
	4f _{5/2} − 5p _{3/2}	E2	113793	87.88	1.068	0.963	3.304[02]	
4f _{7/2}	4f _{7/2} − 4f _{5/2}	M1	1290	7752	1.851	1.851	2.480[-02]	6.30[-04] s
	4f _{7/2} − 5p _{3/2}	E2	115083	86.89	2.635	2.371	1.589[03]	
In-like Ce ⁹⁺								
5p _{3/2}	5p _{3/2} − 5p _{1/2}	M1	33427	299.2	1.151	1.151	3.335[02]	3.00[-03] s
	5p _{3/2} − 5p _{1/2}	E2	33427	299.2	2.175	2.040	4.860[00]	
4f _{5/2}	4f _{5/2} − 5p _{1/2}	E2	54947	182.0	1.277	1.146	1.229[01]	8.12[-02] s
	4f _{5/2} − 5p _{3/2}	E2	21520	464.7	0.679	0.615	3.260[-02]	
4f _{7/2}	4f _{7/2} − 4f _{5/2}	M1	2573	3887	1.851	1.851	1.968[-01]	2.18 s
	4f _{7/2} − 5p _{3/2}	E2	24093	415.1	1.677	1.518	2.620[-01]	
In-like Pr ¹⁰⁺								
4f _{5/2}	4f _{5/2} − 5p _{1/2}	E2	3702	2701	1.062	0.955	1.183[-05]	1.0 day
4f _{7/2}	4f _{7/2} − 4f _{5/2}	M1	3329	3004	1.851	1.851	4.260[-01]	2.35 s
5p _{3/2}	5p _{3/2} − 5p _{1/2}	M1	39141	255.5	1.151	1.151	5.352[02]	1.83[-03] s
	5p _{3/2} − 5p _{1/2}	E2	39141	255.5	1.969	1.851	8.810	
	5p _{3/2} − 4f _{5/2}	E2	35439	282.2	0.561	0.509	4.058[-01]	
	5p _{3/2} − 4f _{7/2}	E2	32110	311.4	1.388	1.258	1.512	
In-like Nd ¹¹⁺								
4f _{7/2}	4f _{7/2} − 4f _{5/2}	M1	4180	2392.3	1.851	1.851	8.434[-01]	1.19 s
5p _{1/2}	5p _{1/2} − 4f _{5/2}	E2	53684	186.3	0.902	0.811	1.641[01]	6.09[-02] s
5p _{3/2}	5p _{3/2} − 5p _{1/2}	M1	45382	220.4	1.150	1.150	8.336[02]	8.76[-04] s
	5p _{3/2} − 5p _{1/2}	E2	45382	220.4	1.790	1.685	1.530[01]	
	5p _{3/2} − 4f _{5/2}	E2	99066	100.9	0.474	0.430	4.938[01]	
	5p _{3/2} − 4f _{7/2}	E2	94886	105.4	1.173	1.064	2.436[02]	

presented in Table V.

In order to evaluate the accuracy of our values, we carried out several calculations which allowed us to separate the effect of higher orders of MBPT, Breit interaction, and contributions of higher partial waves. QED correction is small for transitions with no $5s$ state, and is omitted. The contributions of the higher-orders is evaluated as the difference of the CI+all-order and CI+MBPT

results. The Breit contribution is calculated as the difference of the results with and without the inclusion of this effect. The contribution of the higher ($l > 6$) partial waves (labeled “Extrap”) is estimated to be equal to the contribution of the $l = 6$ partial wave following our empiric rule obtained for Ag-like ions. The contribution of the $l = 6$ partial wave is obtained as the difference of two calculations where all intermediate sums in the

TABLE IX: Comparison of multipole matrix elements in In-like Pr^{10+} , calculated using SDpT (one-electron) and CI+All (three-electron) methods.

	Transition	Energy	λ	Z^{SDpT}	$Z^{\text{CI+all}}$	
					One-el.	Three-el.
M1	$4f_{5/2} \rightarrow 4f_{7/2}$	3329	3004	1.85064	1.85045	1.85045
E3	$4f_{5/2} \rightarrow 4f_{7/2}$	3329	3004	0.29479	0.29157	0.29157
M1	$4f_{5/2} \rightarrow 5p_{3/2}$	35439	282.2	0.00012	0.00006	0.00006
E2	$4f_{5/2} \rightarrow 5p_{3/2}$	35439	282.2	0.50920	0.51700	0.51700
E2	$4f_{7/2} \rightarrow 5p_{3/2}$	32110	311.4	1.25759	1.27820	1.27820
E2	$5p_{1/2} \rightarrow 4f_{5/2}$	3702	2701	0.95489	0.96963	0.96963
M1	$5p_{1/2} \rightarrow 5p_{3/2}$	39141	255.5	1.15049	1.15070	1.15070
E2	$5p_{1/2} \rightarrow 5p_{3/2}$	39141	255.5	1.85071	1.87010	1.87010

all-order and MBPT terms are restricted to $l_{\text{max}} = 6$ and $l_{\text{max}} = 5$. The resulting contributions from higher-order Coulomb correlation (difference of the CI+MBPT and CI+all-order calculations), estimated contributions of higher partial waves (above $l > 6$), and Breit interaction are given separately in columns HO, Extrap, and Breit of Table V. The final theoretical results are listed in “CI+all” column.

The experimental results are from [17] for Cs^{6+} and Ba^{7+} and [31] for Ce^{9+} . Wavelengths for transitions to the ground state are given in last two columns in nm. Estimated uncertainties of theoretical calculations are given in column “Unc”. We use Ba^{7+} reference ion to estimate the uncertainties of the Ce^{9+} calculations using the approaches described in the previous sections. The uncertainty is estimated as the sum of the following: (1) difference of the theoretical and experimental energies for the reference ion (Ba^{7+}) and (2) difference in the sum of all four corrections between the reference and the current ion, Ce^{9+} . The resulting uncertainties for the $4f$ states are very close to the actual differences with experiment, while the uncertainty of the $5p$ state is significantly overestimated.

The energies of the $4f$ levels of Pr^{10+} are very difficult to calculate accurately since these are very close to the ground $5p_{1/2}$ state. The one-electron removal energies of the $5p_{1/2}$ and $4f_{5/2}$ states are $-1.3 \times 10^6 \text{ cm}^{-1}$, and these values cancel to 99.7 % when two energies are subtracted to obtain the *ab initio* transition energy of 3432 cm^{-1} . Meanwhile, all of the corrections (HO, Breit, and Extrap) are large, $1000\text{-}3000 \text{ cm}^{-1}$ and partially cancel each other. Studying the trends of the difference between theory and experiment for three previous ions of the sequence shows that the discrepancy somewhat increases for heavier ions, which probably results from rapid increase of actual removal energies. Therefore, we adjust our *ab initio* values 3432 cm^{-1} and 6761 cm^{-1} for the $4f_{5/2}$ and $4f_{7/2}$ states, respectively, by the difference of the Ce^{9+} results with experiment, i.e. 270 cm^{-1} . The change in sum of all three corrections between Ce^{9+} and Pr^{10+} is only $120\text{-}170 \text{ cm}^{-1}$. Therefore, we estimate the uncertainty in these energies to be on the order of

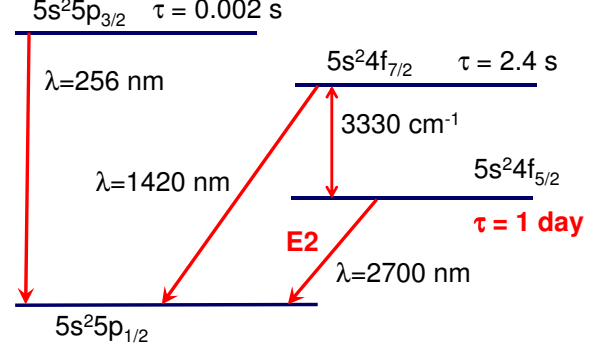


FIG. 2: Energy levels and radiative lifetimes of low-lying levels of In-like Pr^{10+} .

200 cm^{-1} . The uncertainty in the $5p_{3/2}$ energy is taken to be 40 cm^{-1} based on the accuracy of this energy for Ce^{9+} ion.

The sensitivity coefficients q for Pr^{10+} obtained in the lowest-order Dirac-Fock (DF+Breit), SDpT, and CI+all-order approximations are given in Table VI in cm^{-1} . The second-column (DF) shows lowest-order results without the Breit interaction. Breit is included in all other calculations. Just as in the case of Ag-like ions, the correlation effect on the values of q is small, $0.3\text{-}1.0\%$. The Breit interaction contributes from -1.3% to -2.7% . The differences between the coefficients q calculated using the CI+all-order and SDpT methods are negligible. The final CI+all-order sensitivity coefficients q for “monovalent” In-like Ce^{9+} , Pr^{10+} , and Nd^{11+} ions are given in Table VII together with the corresponding CI+all-order transition energies and K enhancement factors.

Lowest-order (Z^{DF}) and all-order (Z^{SDpT}) multipole matrix elements $E2$ and $M1$, transition rates A (in s^{-1}), and lifetimes in In-like ions are listed in Table VIII. The lifetimes are given in the same row as the level designation for the convenience of presentation. Experimental energies from Refs. [17, 31] are used for Cs^{6+} , Ba^{7+} , and Ce^{9+} ions; theoretical energies from Table V are used for Pr^{10+} and Nd^{11+} . Energies (in cm^{-1}) and wavelengths (in nm) are listed for reference. Multipole matrix elements are evaluated by the SDpT method. We have verified that all other transitions give negligible contributions to the lifetimes. Comparison of multipole matrix elements in In-like Pr^{10+} calculated using the SDpT (one-electron) and CI+All (three-electron) methods is given in Table IX. The values calculated by both methods are in excellent agreement. The low-lying levels of Pr^{10+} ion and our estimates of the radiative lifetimes are shown in Fig. 2 for illustration.

The order of levels changes again for Sm^{13+} , where $5s4f^2$ configuration becomes the closest to the ground $5s^24f_j$ fine-structure multiplet. This leads to a very interesting level structure with a metastable $5s4f^2 J = 7/2$ level in the optical transition range to both ground and

TABLE X: Energies of In-like “trivalent” Sm^{13+} and Eu^{14+} ions relative to the ground state calculated using the CI+all-order method (in cm^{-1}). Contributions from higher-order Coulomb correlation (difference of the CI+MBPT and CI+all-order calculations), estimated contributions of higher partial waves (above $l > 6$), Breit interaction, and QED are given separately in columns HO, Extrap, Breit, and QED. Estimated uncertainties of theoretical calculations are given in column “Unc”. Wavelengths for transitions to the ground state are given in the last column in nm.

Level	J	CI+MBPT	HO	Extrap	Breit	QED	Final	Unc.	λ_{th}
Sm^{13+} $5s^24f_{5/2}$ ground state									
$5s^24f$	7/2	6667	-62	7	-440	32	6203	100	1612(28)
$4f^25s$	7/2	21164	2983	-1118	-1626	-1149	20254	940	494(22)
$4f^25s$	9/2	23606	2954	-1117	-1785	-1139	22519	950	444(18)
$4f^25s$	11/2	27339	2893	-1113	-2097	-1119	25904	980	386(14)
$4f^25s$	3/2	30282	2787	-1079	-1599	-1142	29249	900	342(10)
$4f^25s$	13/2	31557	2827	-1108	-2452	-1097	29727	1000	336(11)
$4f^25s$	5/2	31906	2765	-1079	-1720	-1133	30739	900	325(9)
$4f^25s$	7/2	34189	2730	-1079	-1932	-1122	32786	920	305(8)
$4f^25s$	9/2	34418	2864	-1102	-1893	-1135	33152	950	302(8)
$4f^25s$	9/2	36335	2811	-1098	-2048	-1130	34871	950	287(8)
$4f^25s$	7/2	41004	2755	-1085	-1971	-1130	39572	930	253(6)
$4f^25s$	11/2	42079	2873	-1116	-2387	-1130	40319	1000	248(6)
$4f^25s$	5/2	43341	2774	-1082	-1771	-1130	42132	900	237(5)
Eu^{14+} $4f^25s$ $J = 7/2$ ground state									
$4f^3$	9/2	2048	3909	-1074	-1722	-1265	1896	1400	
$4f^25s$	9/2	2785	-27	1	-166	9	2603	130	3842(190)
$4f^3$	11/2	6610	3841	-1073	-2103	-1241	6034	1500	1657(330)
$4f^25s$	11/2	7319	-91	5	-535	33	6732	430	1485(90)
$4f^25s$	3/2	9824	-195	40	36	8	9713	80	1030(9)
$4f^3$	13/2	11316	3773	-1070	-2506	-1219	10294	160	971(130)
$4f^25s$	5/2	11720	-216	40	-245	16	11316	270	884(20)
$4f^25s$	13/2	12361	-159	10	-792	57	11477	400	871(30)
$4f^25s$	9/2	14060	-88	10	-297	20	13705	250	730(13)
$4f^25s$	7/2	14501	-253	40	-349	20	13959	360	716(18)
$4f^3$	15/2	16072	3705	-1067	-2918	-1240	14553	1800	687(75)

TABLE XI: Energies and sensitivity coefficients q for In-like ions relative to the ground state evaluated in the CI+all-order approximation in cm^{-1} ; $K = 2q/\omega$ is the enhancement factor.

Ion	Level	J	Energy	q	K
Sm^{13+}	$5s^24f$	5/2	0	0	
	$5s^24f$	7/2	6203	5654	1.8
	$4f^25s$	7/2	20254	123621	12
	$4f^25s$	9/2	22519	125397	11
	$4f^25s$	11/2	25904	128875	10
	$4f^25s$	3/2	29249	124872	8.5
Eu^{14+}	$4f^25s$	7/2	0	0	
	$4f^3$	9/2	1896	137437	145
	$4f^25s$	9/2	2603	1942	1.5
	$4f^3$	11/2	6034	141771	47
	$4f^25s$	11/2	6732	6293	1.9
	$4f^25s$	3/2	9713	1474	0.3
	$4f^3$	13/2	10294	145723	28

excited $5s^24f_{7/2}$ levels of the fine-structure multiplet. The second level crossing, $5s-4f$, leads to further change of the level order for Eu^{14+} , where $5s4f^2$ becomes the

ground state and the $4f^3$ becomes the first excited level. We note that these levels are very close and the uncertainty of our calculations is comparable to the energy interval. Therefore, it might be possible that $4f^3$ $J = 9/2$ is a ground state configuration. The previous In-like reference ions, such as Ce^{9+} cannot be used to establish the accuracy of the calculations for Sm^{13+} and Eu^{14+} due to completely different set of low-lying configurations. The 25% of all four corrections added in quadrature is used to estimate uncertainty for all levels of Sm^{13+} and $4f^3$ levels of Eu^{14+} . In the case of the $5s^24f$ fine structure multiplet energy levels of Eu^{14+} , we take the average of 25% estimate and sum of the all four corrections as an uncertainty. We note that this is the first time that the CI+all-order method was applied to such complicated configurations as $4f^3$ and no benchmark comparisons with experiment exist for such states. Therefore, experimental measurement of Eu^{14+} will serve as an excellent benchmark of the method accuracy that will allow to further develop the methodology for more complicated systems with partially filled nf shells.

The final CI+all-order sensitivity coefficients q for “trivalent” In-like Sm^{13+} and Eu^{14+} ions are given in

TABLE XII: CI+all-order $Z^{\text{CI+all}}$ multipole matrix elements (in a.u.), transition rates A_r (in s^{-1}), and lifetimes $\tau^{\text{CI+all}}$ (in sec) in In-like Sm^{13+} ion. Energies (in cm^{-1}) and wavelengths (in nm) are from Table X. The numbers in brackets represent powers of 10. CI+all-order matrix elements without RPA correction are listed in column labelled Z^{noRPA} .

Level	Transition			Energy	λ	Z^{noRPA}	$Z^{\text{CI+all}}$	$A_r^{\text{CI+all}}$	$\tau^{\text{CI+all}}$
$5s^2 4f^2 {}^2F_{7/2}$	$5s^2 4f^2 {}^2F_{5/2}$	$5s^2 4f^2 {}^2F_{7/2}$	M1	6203	1612	1.84090	1.84102	2.728[+0]	0.367
	$5s^2 4f^2 {}^2F_{5/2}$	$5s^2 4f^2 {}^2F_{7/2}$	E2	6203	1612	0.21559	0.19504	4.891[-6]	
$5s 4f^2 {}^4H_{7/2}$	$5s^2 4f^2 {}^2F_{5/2}$	$5s 4f^2 {}^4H_{7/2}$	E1	20254	493.7	0.00195	0.00188	7.443[+0]	0.133
	$5s^2 4f^2 {}^2F_{7/2}$	$5s 4f^2 {}^4H_{7/2}$	E1	14051	711.7	0.00033	0.00027	4.949[-2]	
$5s 4f^2 {}^4H_{9/2}$	$5s^2 4f^2 {}^2F_{7/2}$	$5s 4f^2 {}^4H_{9/2}$	E1	16316	612.9	0.00295	0.00275	6.636[+0]	0.141
	$5s^2 4f^2 {}^4H_{7/2}$	$5s 4f^2 {}^4H_{9/2}$	M1	2265	4415	3.85348	3.85331	4.654[-1]	
$5s 4f^2 {}^4H_{11/2}$	$5s 4f^2 {}^4H_{9/2}$	$5s 4f^2 {}^4H_{11/2}$	M1	3385	2954	4.46131	4.46125	1.735[+0]	0.576
$5s 4f^2 {}^4F_{3/2}$	$5s^2 4f^2 {}^2F_{5/2}$	$5s 4f^2 {}^4F_{3/2}$	E1	29249	341.9	0.00384	0.00342	1.484[+2]	6.74[-3]
	$5s^2 4f^2 {}^4H_{7/2}$	$5s 4f^2 {}^4F_{3/2}$	E2	8995	1112	0.45992	0.41986	2.906[-4]	
$5s 4f^2 {}^4H_{13/2}$	$5s 4f^2 {}^4H_{11/2}$	$5s 4f^2 {}^4H_{13/2}$	M1	3823	2616	3.94521	3.94520	1.676[+0]	0.597
$5s 4f^2 {}^4F_{5/2}$	$5s^2 4f^2 {}^2F_{5/2}$	$5s 4f^2 {}^4F_{5/2}$	E1	30739	325.3	0.00321	0.00293	8.426[+1]	9.62[-3]
	$5s^2 4f^2 {}^2F_{7/2}$	$5s 4f^2 {}^4F_{5/2}$	E1	24536	407.6	0.00221	0.00198	1.956[+1]	
	$5s^2 4f^2 {}^4F_{3/2}$	$5s 4f^2 {}^4F_{5/2}$	M1	1490	6711	3.02239	3.02227	1.358[-1]	
$5s 4f^2 {}^4F_{7/2}$	$5s^2 4f^2 {}^2F_{5/2}$	$5s 4f^2 {}^4F_{7/2}$	E1	32786	305.0	0.00304	0.00280	6.993[+1]	1.20[-2]
	$5s^2 4f^2 {}^2F_{7/2}$	$5s 4f^2 {}^4F_{7/2}$	E1	26583	376.2	0.00177	0.00165	1.292[+1]	
	$5s^2 4f^2 {}^4H_{7/2}$	$5s 4f^2 {}^4F_{7/2}$	M1	12532	798.0	0.17400	0.17406	2.011[-1]	
	$5s^2 4f^2 {}^4F_{5/2}$	$5s 4f^2 {}^4F_{7/2}$	M1	2047	4885	3.45771	3.45759	3.457[-1]	
$5s 4f^2 {}^2H_{9/2}$	$5s^2 4f^2 {}^2F_{7/2}$	$5s 4f^2 {}^2H_{9/2}$	E1	26949	371.1	0.01033	0.00948	3.565[+2]	2.78[-3]
	$5s^2 4f^2 {}^4H_{7/2}$	$5s 4f^2 {}^2H_{9/2}$	M1	12898	775.3	0.68327	0.68350	2.704[+0]	
$5s 4f^2 {}^4F_{9/2}$	$5s^2 4f^2 {}^2F_{7/2}$	$5s 4f^2 {}^4F_{9/2}$	E1	28668	348.8	0.00512	0.00461	1.014[+2]	9.61[-3]
	$5s^2 4f^2 {}^4H_{7/2}$	$5s 4f^2 {}^4F_{9/2}$	M1	14617	684.1	0.47303	0.47324	1.887[+0]	
	$5s^2 4f^2 {}^4H_{9/2}$	$5s 4f^2 {}^4F_{9/2}$	M1	12352	809.6	0.31732	0.31751	5.125[-1]	
	$5s^2 4f^2 {}^4F_{7/2}$	$5s 4f^2 {}^4F_{9/2}$	M1	2085	4796	2.17866	2.17854	1.160[-1]	
$5s 4f^2 {}^2G_{7/2}$	$5s^2 4f^2 {}^2F_{5/2}$	$5s 4f^2 {}^2G_{7/2}$	E1	39572	252.7	0.00997	0.00971	1.481[+3]	5.31[-4]
	$5s^2 4f^2 {}^2F_{7/2}$	$5s 4f^2 {}^2G_{7/2}$	E1	33369	299.7	0.00721	0.00649	3.966[+2]	
	$5s^2 4f^2 {}^4H_{7/2}$	$5s 4f^2 {}^2G_{7/2}$	M1	19318	517.7	0.36671	0.36685	3.271[+0]	
	$5s^2 4f^2 {}^4H_{7/2}$	$5s 4f^2 {}^2G_{7/2}$	E2	19318	517.7	0.05726	0.05278	1.049[-4]	
	$5s^2 4f^2 {}^4H_{9/2}$	$5s 4f^2 {}^2G_{7/2}$	M1	17053	586.4	0.31361	0.31357	1.644[+0]	
$5s 4f^2 {}^2H_{11/2}$	$5s 4f^2 {}^4H_{9/2}$	$5s 4f^2 {}^2H_{11/2}$	M1	17800	561.8	0.20453	0.20464	5.309[-1]	0.207
	$5s 4f^2 {}^4H_{13/2}$	$5s 4f^2 {}^2H_{11/2}$	M1	10592	944.1	0.61358	0.61320	1.004[+0]	
	$5s 4f^2 {}^2H_{9/2}$	$5s 4f^2 {}^2H_{11/2}$	M1	7167	1395	1.62570	1.62592	2.188[+0]	
	$5s 4f^2 {}^4F_{9/2}$	$5s 4f^2 {}^2H_{11/2}$	M1	5448	1836	1.66373	1.66384	1.006[+0]	
$5s 4f^2 {}^2F_{5/2}$	$5s^2 4f^2 {}^2F_{5/2}$	$5s 4f^2 {}^2F_{5/2}$	E1	42132	237.3	0.01158	0.01101	3.062[+3]	3.19[-4]
	$5s^2 4f^2 {}^2F_{7/2}$	$5s 4f^2 {}^2F_{5/2}$	E1	35929	278.3	0.00242	0.00214	7.140[+1]	
	$5s^2 4f^2 {}^4F_{3/2}$	$5s 4f^2 {}^2F_{5/2}$	M1	12883	776.2	0.43435	0.43453	1.815[+0]	

Table XI together with the corresponding CI+all-order transition energies and K enhancement factors.

The CI+all-order $Z^{\text{CI+all}}$ multipole matrix elements (E1, E2, E3, M1, M2, and M3), transition rates A_r (in s^{-1}), and lifetimes $\tau^{\text{CI+all}}$ (in sec) in In-like Sm^{13+} ion are listed in Table XII. Energies from Table X used for evaluation of the matrix elements and transition rates are given for reference. Multipole matrix elements are evaluated in the CI+all-order approximations (a.u.). The numbers in brackets represent powers of 10. The CI+all-order matrix elements calculated without random-phase-approximation (RPA) correction are listed in column labelled Z^{noRPA} . In such a calculation, “bare” E_k and

Mk operators are used instead of the effective transition operators (for example electric-dipole D^{eff}). While RPA correction is significant for E1 and E2 transitions, it is small for M1 transitions between the levels of the fine-structure multiplet.

We find that the lifetimes of the Sm^{13+} levels are relatively small, less than 1 sec, making it less attractive for our applications of interest. Nevertheless, shorter lifetimes will make locating the transitions easier so this ion may be used as a benchmark for further improvement of the theory. If measurements are carried out in this ion, it may be possible to use the resulting comparison to further improve the theory for other ions.

The case of Eu^{14+} is similar and does not appear to have all features for the clock development. While uncertainty of our data is large, present results place the first level too close to the ground state to be practically useful. The next level is of the same configuration as the ground state and has small value of q . Finally, $4f^3 J = 11/2$ level is short lived since it can decay via the $M1$ transition to $4f^3 J = 9/2$ level below. However, measurement of this ion energy levels would be very useful as the benchmark for other systems.

V. CONCLUSION

We carried out detailed high-precision study of Ag-like Nd^{13+} and Sm^{15+} and In-like Ce^{9+} , Pr^{10+} , Nd^{11+} , Sm^{13+} , and Eu^{14+} highly-charged ions for future experimental studies aimed at the development of ultra-precise atomic clocks and search for α -variation. The energies of Nd^{13+} , Sm^{15+} and In-like Ce^{9+} ions were found to be

in excellent agreement with experiment. The energies, transition wavelengths, electric- and magnetic-multipole reduced matrix elements, lifetimes, and sensitivity coefficients to α -variation q and K were calculated. Several methods were developed to evaluate uncertainties of the results. Particular interesting cases for experimental exploration were highlighted.

Acknowledgement

We thank C. W. Clark, C. Monroe, J. Tan, Yu. Ralchenko, and P. Beiersdorfer for useful discussions. M.S.S. thanks School of Physics at the University of New South Wales, Sydney, Australia for hospitality and acknowledges support from Gordon Godfrey Fellowship, UNSW. This work was supported in part by US NSF Grant No. PHY-1212442. M.G.K. acknowledges support from RFBR Grant No. 14-02-00241. The work was partly supported by the Australian Research Council.

-
- [1] J.-P. Uzan, Rev. Mod. Phys. **75**, 403 (2003).
 - [2] J. K. Webb, J. A. King, M. T. Murphy, V. V. Flambaum, R. F. Carswell, and M. B. Bainbridge, Phys. Rev. Lett. **107**, 191101 (2011).
 - [3] J. C. Berengut and V. V. Flambaum, Europhys. Lett. **97**, 2006 (2012).
 - [4] J. C. Berengut, V. V. Flambaum, and A. Ong, Eur. Phys. J. Web of Conferences **57**, 02001 (2013).
 - [5] T. Rosenband, D. B. Hume, P. O. Schmidt, C. W. Chou, A. Brusch, L. Lorini, W. H. Oskay, R. E. Drullinger, T. M. Fortier, J. E. Stalnaker, et al., Science **319**, 1808 (2008).
 - [6] N. Hinkley, J. A. Sherman, N. B. Phillips, M. Schioppa, N. D. Lemke, K. Beloy, M. Pizzocaro, C. W. Oates, and A. D. Ludlow, Science **341**, 1215 (2013).
 - [7] B. J. Bloom, T. L. Nicholson, J. R. Williams, S. L. Campbell, M. Bishof, X. Zhang, W. Zhang, S. L. Bromley, and J. Ye, Nature **506**, 71 (2014).
 - [8] J. C. Berengut, V. A. Dzuba, and V. V. Flambaum, Phys. Rev. Lett. **105**, 120801 (2010).
 - [9] J. C. Berengut, V. A. Dzuba, V. V. Flambaum, and A. Ong, Phys. Rev. Lett. **106**, 210802 (2011).
 - [10] V. A. Dzuba, A. Derevianko, and V. V. Flambaum, Phys. Rev. A **86**, 054502 (2012).
 - [11] M. S. Safronova, V. A. Dzuba, V. V. Flambaum, U. I. Safronova, S. G. Porsev, and M. G. Kozlov, Phys. Rev. Lett. **113**, 030801 (2014).
 - [12] A. Derevianko, V. A. Dzuba, and V. V. Flambaum, Phys. Rev. Lett. **109**, 180801 (2012).
 - [13] M. S. Safronova and W. R. Johnson, Adv. At. Mol. Opt. Phys. **55**, 191 (2008).
 - [14] G. E. Brown and D. G. Ravenhall, Proc. R. Soc. London, Ser. A **208**, 552 (1951).
 - [15] S. A. Blundell, W. R. Johnson, Z. W. Liu, and J. Sapirstein, Phys. Rev. A **40**, 2233 (1989).
 - [16] V. V. Flambaum and J. S. Ginges, Phys. Rev. A **72**, 052115 (2005).
 - [17] Yu. Ralchenko, F.-C. Jou, D. E. Kelleher, A. E. Kramida, A. Musgrove, J. Reader, W. L. Wiese, and K. Olsen (2005). NIST Atomic Spectra Database (version 3.0.2), [Online]. Available: <http://physics.nist.gov/asd3> [2006, January 4]. National Institute of Standards and Technology, Gaithersburg, MD.
 - [18] J. Sugar and V. Kaufman, Phys. Scripta **24**, 742 (1981).
 - [19] M. G. Kozlov, Int. J. Quant. Chem. **100**, 336 (2004).
 - [20] M. S. Safronova, M. G. Kozlov, W. R. Johnson, and D. Jiang, Phys. Rev. A **80**, 012516 (2009).
 - [21] V. A. Dzuba, V. V. Flambaum, and M. G. Kozlov, Phys. Rev. A **54**, 3948 (1996).
 - [22] M. S. Safronova, M. G. Kozlov, and C. W. Clark, Phys. Rev. Lett. **107**, 143006 (2011).
 - [23] S. G. Porsev, M. S. Safronova, and M. G. Kozlov, Phys. Rev. Lett. **108**, 173001 (2012).
 - [24] M. S. Safronova, S. G. Porsev, M. G. Kozlov, and C. W. Clark, Phys. Rev. A **85**, 052506 (2012).
 - [25] M. S. Safronova, M. G. Kozlov, and C. W. Clark, IEEE Transactions on Ultrasonics, Ferroelectrics, and Frequency Control **59**, 439 (2012).
 - [26] M. S. Safronova, M. G. Kozlov, and U. I. Safronova, Phys. Rev. A **85**, 012507 (2012).
 - [27] M. S. Safronova, S. G. Porsev, and C. W. Clark, Phys. Rev. Lett. **109**, 230802 (2012).
 - [28] M. S. Safronova, W. R. Johnson, U. I. Safronova, and T. E. Cowan, Phys. Rev. A **74**, 022504 (2006).
 - [29] M. S. Safronova and U. I. Safronova, Phys. Rev. A **83**, 052508 (2011).
 - [30] P. J. Mohr, B. N. Taylor, and D. B. Newell (2011), "The 2010 CODATA Recommended Values of the Fundamental Physical Constants" (Web Version 6.0). This database was developed by J. Baker, M. Douma, and S. Kotochigova. Available: <http://physics.nist.gov/constants>. NIST, Gaithersburg, MD 20899.
 - [31] Y. N. Joshi, A. N. Ryabtsev, and S. S. Churilov, Phys. Scripta **64**, 326 (2001).

- [32] M. S. Safronova and P. K. Majumder, Phys. Rev. A **87**, 042502 (2013).
Rev. A **87**, 032513 (2013).
- [33] M. S. Safronova, U. I. Safronova, and S. G. Porsev, Phys.